_Q. 2088_

Y-2165

MASTER

INERTIA AND FRICTION WELDING OF TYPE 1100 ALUMINUM TO TYPE 316 STAINLESS STEEL

M. A. Perkins

December 1978

UNION CARBIDE

OAK RIDGE Y-12 PLANT
OAK RIDGE, TENNESSEE

DISCLAIMER

This report was prepared as an account of work sponsored by an agency of the United States Government. Neither the United States Government nor any agency Thereof, nor any of their employees, makes any warranty, express or implied, or assumes any legal liability or responsibility for the accuracy, completeness, or usefulness of any information, apparatus, product, or process disclosed, or represents that its use would not infringe privately owned rights. Reference herein to any specific commercial product, process, or service by trade name, trademark, manufacturer, or otherwise does not necessarily constitute or imply its endorsement, recommendation, or favoring by the United States Government or any agency thereof. The views and opinions of authors expressed herein do not necessarily state or reflect those of the United States Government or any agency thereof.

DISCLAIMER

Portions of this document may be illegible in electronic image products. Images are produced from the best available original document.

INERTIA AND FRICTION WELDING OF TYPE 1100 ALUMINUM TO TYPE 316 STAINLESS STEEL

M. A. Perkins

Metallurgy Department
Y-12 Development Division

2

ABSTRACT

The inertia and friction-welding processes were evaluated for joining Type 1100-H14 aluminum to Type 316 VIM VAR stainless steel. While both processes consistently produce joints whose strength exceed the aluminum base metal, 100 percent bonding has not been reliably achieved. This difficiency points out the need for the development of nondestructive testing techniques for this type of joint. Additionally, solid-state volume diffusion did not appear to be a satisfactory explanation for the inertia and friction-welding bonding mechanism.

CONTENTS

4

SUMMARY

This evaluation of friction and inertia welding indicates that welds can be made between Type 1100 aluminum and Type 316 stainless steel. From a purely mechanical standpoint, the strength of these bonds will consistently exceed the strength of the aluminum base metal. However, 100 percent bonding was not reliably achieved, and this fact points out the need for nondestructive testing methods that will ascertain the degree of bonding. While nondestructive testing of dissimilar metal joints has been encouraging, the work has yet to reach fruition.

This evaluation did not shed much light on a possible bonding mechanism for friction and inertia welding. Solid-state, volume diffusion was not a satisfactory explanation for the degree of iron and chromium migration detected in this work; and, thus, mechanical mixing might be more likely. However, no evidence of mechanical mixing was detected. Additionally, no evidence of melting, as recently reported by others, was detected.

INTRODUCTION

The occasional need for aluminum/stainless steel transition joints led to an investigation of the inertia and friction-welding processes as a means for joining Type 1100-H14 aluminum to Type 316 VIM VAR (vacuum-induction-melted, vacuum-arc-remelted) stainless steel. Inertia and friction welding are solid-state welding processes wherein coalescence is produced after heating is obtained from a mechanically induced sliding motion between rubbing surfaces held together under pressure. The friction-welding process is based on rotating one part at a relatively high constant speed against the stationary member to which it is to be joined. After a preset period of time, a brake is applied, the rotation stopped, and a predetermined forge pressure applied. The contacting surfaces are thus heated by friction to a high temperature and forged together to produce a reliable, high-strength weld. Inertia welding differs from friction welding in that all the kinetic energy for welding is stored in a revolving flywheel/spindle system. After the energy is stored, the flywheel is disengaged and the flywheel energy is consumed by the weld. The weld is made by the same sequence of events as friction welding except that the flywheel is continually decelerating and no brake is used to stop it.[1-3]

While general experience and information is available for inertia and friction welding aluminum/stainless steel combinations, the Type 316 VIM VAR stainless steel-to-Type 1100-H14 aluminum combination is unique in that it is potentially one of the most difficult combinations to weld since there is such a wide dissimilarity in strength when compared to other aluminum/stainless steel combinations.

This study was conducted at the Oak Ridge Y-12 Plant.[a]

(a) Operated by the Union Carbide Corporation's Nuclear Division for the Department of Energy.

TWO METHODS FOR WELDING ALUMINUM TO STAINLESS STEEL

INERTIA WELDING

Material

Material for the inertia-welding evaluation was secured in the form of 12.7-mm-diameter rod stock. The Type 1100 aluminum was obtained in the half-hard condition (1100-H14) to narrow the disparity in strength between it and the stainless steel. The Type 316 VIM VAR stainless steel, which is a high-quality, low-inclusion stainless steel, resulting from vacuum-induction-melted (VIM), vacuum-arc-remelted(VAR) processing, was also obtained as 12.7-mm-diameter rod stock.

Welding

Recent work had indicated that in friction welding hard/soft metal combinations, where there is plastic flow of only the soft metal during welding, surface geometries (other than flat) on the hard metal will aid in metal flow and produce superior weld joints.[4] This belief led to the selection of three stainless steel surface geometries for evaluation: (1) a flat surface, (2) a cone with a 150-degree included angle, and (3) a curved surface with a 25.4-mm radius. All aluminum samples had a flat surface. These three types of joints are depicted in Figure 1. All samples had a 0.85-μm surface finish, a finish that was determined to be optimum in recent work completed at the British Welding Institute.[5]
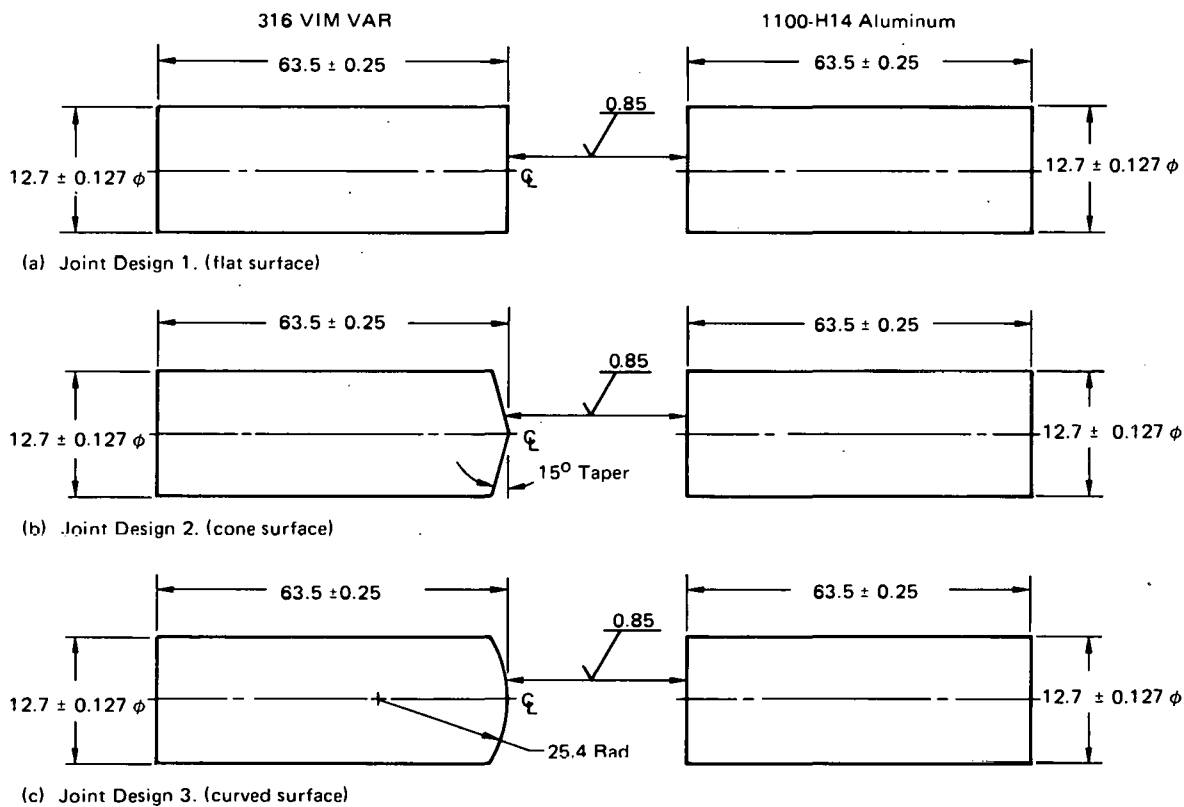

Figure 1. THREE INERTIA-WELD-JOINT DESIGNS FOR EVALUATION. (All Dimensions are in mm)

The program was initiated by determining the optimum inertia welding parameters[b] for 12.7-mm-diameter Type 316 VIM VAR stainless steel/Type 1100-H14 aluminum. These parameters were determined with flat-surfaced samples (Figure 1, Joint Design 1) since this was considered to be the most difficult geometry to weld. With the use of the hammer bend test (a frequently used screening test for friction welds[6]) as an evaluation, the following parameters were developed:

Moment of Inertia - 0.055 kg m^2
Welding Speed   - 4000 rpm
Welding Force   - 3.6 kN
Upset Speed   - 100 rpm
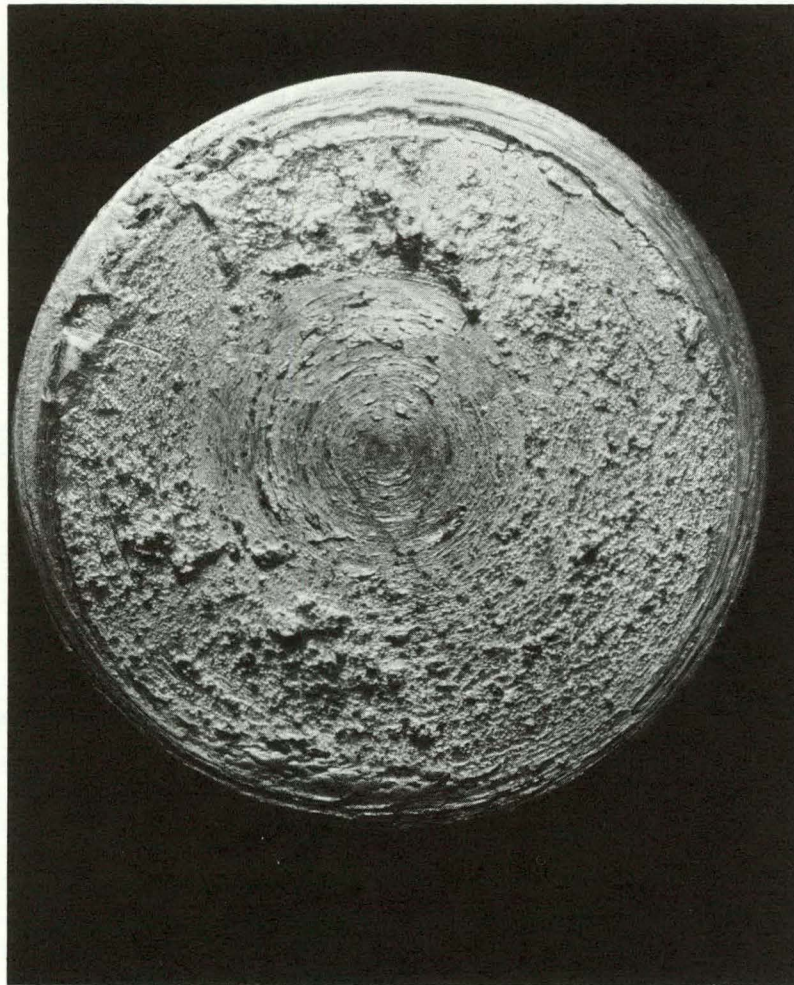Upset Force   - 8.2 kN

Figure 2 presents photomacrographs of one of the welds made during this parameter development study. The sample was intentionally broken at the interface to examine the stainless steel surface for aluminum adherence which, as can be seen, was good. Stainless steel preparation prior to welding consisted of degreasing the surface to be welded with alcohol and a soft tissue. Aluminum preparation consisted of cleaning the surface to be welded in a bright dip solution of 85 vol % phosphoric acid, 3 vol % nitric acid, and 12 vol % water for one minute at 60° C, rinsing in warm water, and wiping with alcohol and a soft tissue.

These parameters and cleaning procedures were then used to weld a series of six each of the three different joint designs in Figure 1. In order to monitor the inertia welding parameters, oscillograph traces were made of the principal welding parameters: flywheel speed, force, and upset distance, and the length of travel during the welding process. Figure 3 is a typical oscillograph trace. It was hoped that, in this manner, differences which might occur in the evaluation of the welds could be correlated to subtle differences in the oscillograph traces.

Evaluation

The six welds of each of the three joint designs were evaluated by machining five of the welds into tensile specimens and designating one weld for metallographic examination. One drawback to the tensile test as a means of evaluation is that it is a test of joint strength and not a test of bond strength because a characteristic of the tensile tests on joints between materials with very different strengths is that the strain is localized in the weaker metal away from the joint. When uniaxial tensile loading is applied to a dissimilar metal specimen, a triaxial stress system is set up in the softer material close to the interface where the material is not free to undergo radial strain. Triaxial yield stress is greater than uniaxial yield stress; so, provided the soft material has sufficient ductility, plastic strain and failure occur away from the triaxial stress field.[7] However, the tensile test was still chosen because it was felt that the influence of the different joint geometries would severely complicate the results

---

(b) The welding was done on a Model 90 Caterpillar inertia welder.

(a) Top View.   M320a

(b) Side View.   M320b

Figure 2. TWO VIEWS OF THE STAINLESS STEEL INTERFACE OF A 316 VIM VAR/TYPE 1100-H14 ALUMINUM INERTIA WELD. (8X)

of the more quantitative static shear test recommended by the British Welding Institute for evaluating dissimilar metal joints. Their work has been limited to welds which incorporate only the flat-surfaced joint geometry.
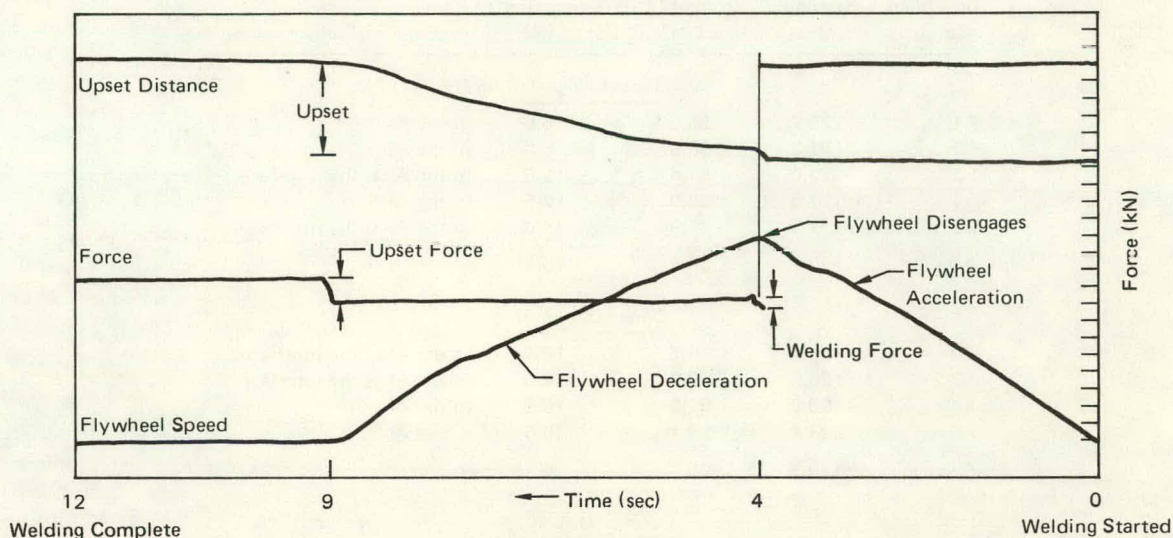

Figure 3. OSCILLOGRAPH TRACE OF THE INERTIA WELDING PARAMETERS FOR WELD A3. (1 Division = 8.2 kN Force, 350 rpm, 0.86-mm Upset)

Table 1 lists the results of the tensile tests. As these results indicate, the cone design (Joint Design 2) demonstrated a slightly higher strength than the other two designs.

Two different modes of failure were encountered in the tensile specimens, as described in Table 1, with an apparent effect on the joint elongation. In one case, the specimens necked and failed in the aluminum base metal; while, in the other case, the specimens necked in the aluminum base metal but partially failed at the joint interface, revealing areas of apparent lack of bonding. Figure 4 reveals the two conditions. Figures 5 and 6 present the results of a scanning electron microscope evaluation which tends to verify the existence of unbonded areas. The oscillograph traces of these welds failed to reveal any differences.

The potential presence of unbonded areas, which can only be detected by destructive tests, points to the need for a nondestructive test method for these types of joints.

Figures 7 and 8 are representative photomacrographs and photomicrographs of the weld and weld interface of an inertia weld which incorporated Joint Design 2 (Figure 1). Metallographic examination revealed nothing unusual and the intermetallic compound ($FeAl_3$), as seen by other investigators, was not detected. Figure 9 shows the results of point-counting, electron-microprobe scans of this same weld interface. These results indicate significant iron and chromium penetration into the aluminum for a distance of 4 μm, with less significant penetration for an additional 2 μm. No penetration of the aluminum into the stainless steel was detected.

Table 1

TENSILE-TEST RESULTS FOR INERTIA WELDS
(316 VIM-VAR Stainless Steel/1100-H14 Aluminum)

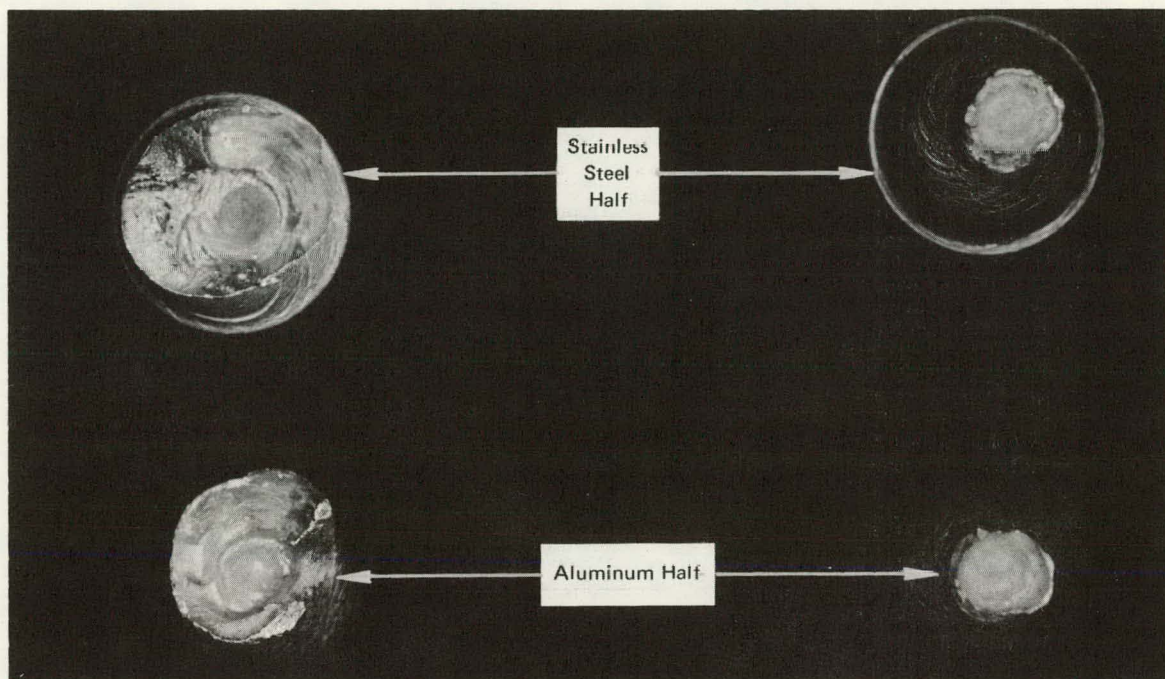| Specimen Number	Tensile Strength (MPa)	Yield Strength[1] (MPa)	Elongation[2] (%)	Location of Failure
Flat (Design 1)				
F1	120.7	86.9	15.0	In the Al.
F2	121.3	86.9	16.5	In the Al.
F3	122.0	87.6	12.5	In the Al at the interface.
F4	117.9	80.0	17.5	In the Al.
F5	121.3	86.9	14.0	In the Al at the interface.
Average	120.7	85.6	15.1	
Cone (Design 2)				
A2	123.4	96.5	10.0	In the Al at the interface.
A3	126.9	97.9	8.5	In the Al at the interface.
A4	128.9	91.0	10.5	In the Al.
A5	123.4	95.1	10.0	In the Al.
Average	125.7	95.1	9.75	
Curved (Design 3)				
R2	122.7	89.6	15.5	In the Al.
R3	122.7	93.8	7.5	In the Al at the interface.
R4	124.1	92.4	15.0	In the Al.
R5	124.8	95.1	10.0	In the Al at the interface.
R6	120.7	88.3	15.0	In the Al.
Average	123.0	91.8	12.6	

(1) At 0.2% offset.
(2) In 25.4 mm.

There is considerable debate among researchers as to the exact nature of the bonding mechanism in both inertia and friction welding. The proposed mechanisms range from solid-state diffusion to mechanical mixing.[8] It appears highly unlikely that volume diffusion in the solid state is the bonding mechanism due to the extremely short welding times. The amount of solid-state, volume diffusion which could occur during a typical inertia weld can be calculated as:

$$x = \sqrt{Dt},$$

where x represents the distance of migration, in centimeters; D, the diffusion coefficient; and t, the time. Using the diffusion coefficient for the volume diffusion of iron in aluminum (for the temperature range of 580 to 660° C), as determined by Hood[9] and verified by Tiwari and Sharma:[10]
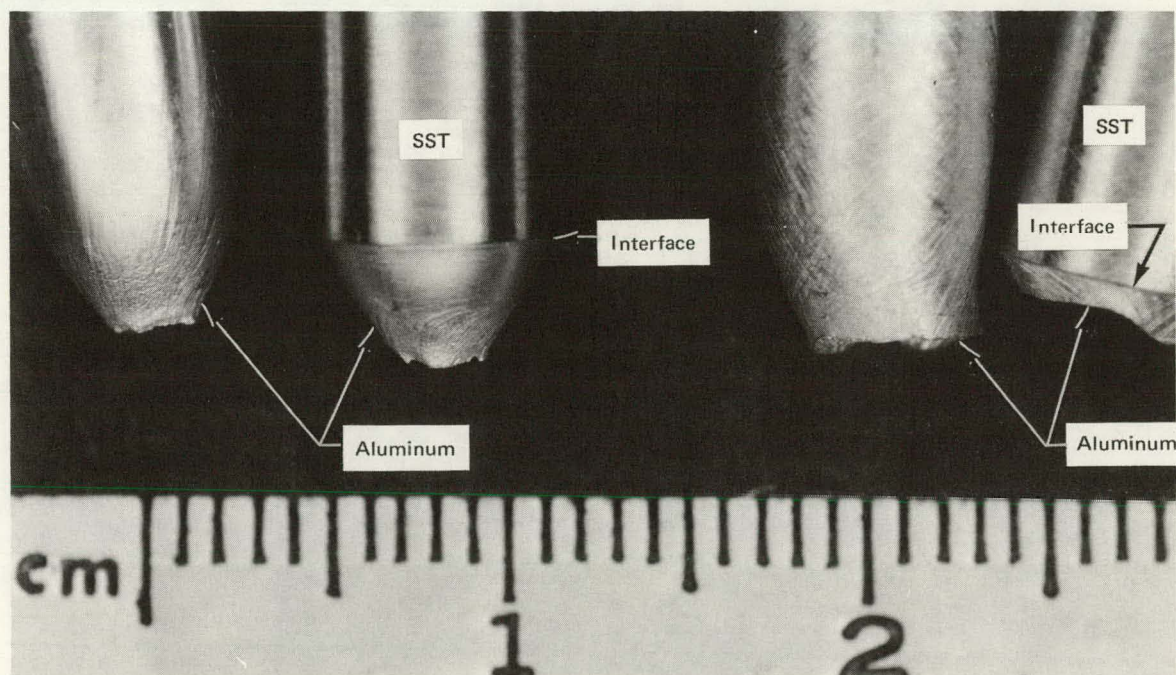
$$D = 9.1 \times 10^5 \exp\left(-\frac{2.68 \, eV}{kT}\right) cm^2/sec,$$

and at a welding-cycle time of three seconds for the inertia welder, the expression becomes:

(a) Top View.

M340a

(b) Side View.

M340b

Figure 4. PHOTOMACROGRAPHS THAT SHOW THE TWO MODES OF TENSILE FAILURE IN 316 VIM VAR STAINLESS STEEL/1100-H14 ALUMINUM INERTIA WELDS. (5X)

SM-63674   SM-63679   SM-63683

Figure 5. SCANNING ELECTRON MICROSCOPE MONTAGE OF THE FAILED STAINLESS STEEL SURFACE OF SPECIMEN A3. (Areas which are Void of any Aluminum Adherence are Evident when Compared with Figure 6; ~ 7X)

SM-63873   SM-63880   SM-63884

Figure 6. SCANNING ELECTRON MICROSCOPE ALUMINUM X-RAY MAP THAT VERIFIES THOSE AREAS WHICH ARE VOID OF ALUMINUM (THE DARK AREAS). (This Area is the same as that in Figure 5; ~ 70X)

13

MS-76-0677-1

Figure 7. PHOTOMACROGRAPH OF THE INERTIA WELD THAT INCORPORATED JOINT DESIGN 2. (4X)

MS-76-0677-2

Figure 8. PHOTOMICROGRAPH OF THE INTERFACE OF AN INERTIA WELD THAT INCORPORATED JOINT DESIGN 2. (Polished and Etched; Bright Field Illumination; 50X)

$$x = \sqrt{9.1 \times 10^5 \exp\left(-\frac{2.68 \text{ eV}}{kT}\right) \text{cm}^2/\text{sec [3 sec]}}.$$

A cycle time of three seconds is that period of time during which the stainless steel and aluminum surfaces are presented for bonding and held under the upset force (Figure 3). Prior to this time, upset of the aluminum workpiece is continually presenting a new surface to the stainless steel and only heating is occurring. Assuming that the maximum temperature during this welding cycle approaches the melting point of aluminum (660° C), and substituting:

Figure 9. RESULTS OF MICROPROBE SCANS OF THE INTERFACE OF A TYPE 1100-H14 ALUMINUM/316 VIM VAR STAINLESS STEEL INERTIA WELD. (Zero Distance is the Approximate Weld Interface)

$$x = \sqrt{9.09 \times 10^{-9} \text{ cm}^2}, \text{ or}$$

$$x = 9.5 \times 10^{-5} \text{ cm}.$$

Thus, approximately 950 nm of iron diffusion into aluminum is possible under these conditions. Using a value of:

$$D = 2.4 \times 10^3 \exp\left(-\frac{2.65 \text{ eV}}{kT}\right) \text{cm}^2/\text{sec}$$

for the volume diffusion of chromium in aluminum[9] and the same conditions, the extent of diffusion would be:

$$x = 5.9 \times 10^{-6} \text{ cm},$$

or there would be 59 nm of chromium diffusion into aluminum. Under these conditions, a welding cycle time of nearly 60 seconds is necessary to produce 4 μm of iron diffusion, and even longer times are necessary for the chromium diffusion. These calculations then verify that solid-state, volume diffusion is not a satisfactory explanation for the extent of iron and chromium penetration revealed by the microprobe scans.[11] The fact that equivalent iron and chromium penetration (4 μm) was detected may be an indication that mechanical mixing is the bonding mechanism.

Iron and chromium penetration into aluminum during friction and inertia welding of aluminum and stainless steel (exceeding that possible by solid-state, volume diffusion) has been reported.[12-14] None of these investigators, however, have made a definitive statement as to the cause. Recently, one investigator has suggested that all solid-state welding processes, including friction welding, result in melting on the micrometer-to-
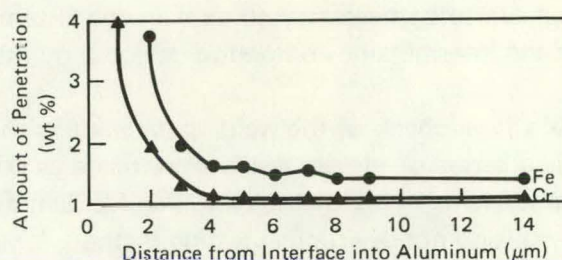
submicrometer scale.[15] While this particular search for evidence of melting in friction welds was not very fruitful, evidence of mechanical mixing was found. Mechanical mixing may explain the bonding mechanism in inertia and friction welds; however, the presence of liquid metal, which would increase the diffusion coefficient by several orders of magnitude, appears to be necessary to explain the extent of iron and chromium penetration and layers of the intermetallic compound detected by others.

As a final check of the welding parameters and the cone joint design (Joint Design 2, Figure 1), a series of eleven welds were made as control samples. Table 2 presents the results of these welds. Two of the eleven welds demonstrated lack of bonding, again supporting the need for a nondestructive testing method.

Table 2

TENSILE-TEST RESULTS FOR CONTROL SAMPLES
(316 VIM VAR Stainless Steel/1100-H14 Aluminum)

Specimen Number	Tensile Strength (MPa)	Yield Strength[1] (MPa)	Elongation[2] (%)	Location of Failure
1	113.1	82.7	17.5	In the Al base metal.
2	115.1	84.1	17.0	In the Al base metal.
3	113.8	82.7	18.5	In the Al base metal.
4	111.0	79.3	18.0	In the Al base metal.
5	112.4	81.4	18.5	In the Al base metal.
6	115.1	86.9	18.5	In the Al base metal.
7	113.1	87.6	7.0	In the Al at the interface.
8	107.6	86.2	9.0	In the Al at the interface.
9	113.1	86.9	18.0	In the Al base metal.
10	117.2	84.1	18.0	In the Al base metal.
11	111.7	79.3	18.5	In the Al base metal.
Mean	113.0	83.8	16.2	
1s Confidence Level	± 2.5	± 3.0	± 4.1	

(1) At 0.2% offset.
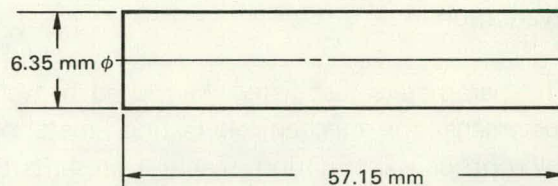(2) In 25.4 mm.

FRICTION WELDING

Material

Material for the friction-welding evaluation was secured in the form of 6.35-mm-diameter Type 1100-H14 rod stock and 3.175-mm-OD, 1.067-mm-ID Type 316 VIM VAR stainless steel tubing. These were the maximum sizes which the friction welder could accommodate. Figure 10 depicts the piece parts for the friction welding and includes the 15-degree taper and 0.85-μm finish on the stainless steel which had been used successfully in the inertia-welding evaluation.

Welding

Welding was done on a microfriction welder[c] which had undergone some minor modifications. To develop a set of welding parameters, a series of welds, using the piece-part design depicted in Figure 10, were made at varying parameters. The piece-part cleaning was the same as that for the inertia welding. After welding, the samples (two at each set of parameters) were machined to 3.18-mm rods and evaluated by subjecting one weld to a bend test and the other to a tensile test. For the bend test, the weld was bent around a mandrel which was three times the work-piece diameter. Table 3 summarizes these data. While all of the tensile specimens

(a) 1100-H14 Aluminum.

(b) 316 VIM VAR Stainless Steel.

Figure 10. DESIGN OF THE FRICTION-WELD PIECE PARTS AND WELD JOINT.

failed in the aluminum away from the bond interface, the bend tests proved to be very revealing. The bend test provided data by which to rate the welding parameters and revealed unbonded areas in some of the specimens. As a result of these data, the following parameters were chosen for further investigation: a welding speed of 60,000 rpm, a welding force of 667 N, and an upset distance of 0.5 mm.

Table 3

EVALUATION OF THE FRICTION WELDING PARAMETERS

| | Friction Welding Parameters | | | Evaluation | | |
Sample Number	Welding Speed (rpm)	Welding Force (N)	Upset Distance (mm)	Ultimate Tensile Strength (MPa)	Bend Angle (deg)	Remarks
1	40,000	445	0.5	137.9	> 90	
2	40,000	556	0.5	137.1	< 45	
3	40,000	667	0.5	131.3	< 45	Unbonded area in the bend specimen.
4	40,000	778	0.3	131.3	< 45	Unbonded area in the bend specimen.
5	50,000	556	0.5	130.7	< 90	
6	50,000	778	0.3	134.6	-	Bend specimen failed in machining.
7	60,000	667	0.3	130.7	> 90	
8	60,000	667	0.5	129.1	> 90	
9	70,000	667	0.5	135.7	> 45	

Evaluation

The parameters just listed were used to weld a series of specimens for mechanical testing, metallography, and microprobe examination. Table 4 presents the results of the mechanical tests. All of the tensile specimens failed in the aluminum base metal and all of the bend specimens exceeded 90 degrees. These specimens were prepared for testing in the manner previously mentioned.
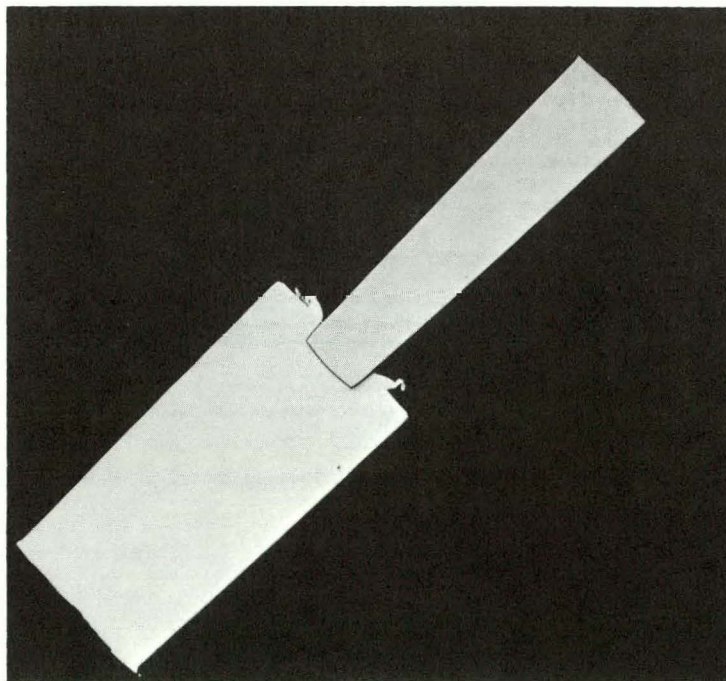
Figures 11 and 12 are representative photomacrographs and photomicrographs of the friction weld and weld interface. Metallographic examination revealed nothing unusual; and, again, the intermetallic compound ($FeAl_3$) was not detected. Figure 13 shows the results of point-counting electron-microprobe scans made across the weld interface. These results indicate significant iron and chromium penetration (5 μm) into the aluminum, with less significant penetration for approximately an additional 6 μm. No penetration of the aluminum into the stainless steel was detected.

Table 4

TEST RESULTS OF FRICTION-WELDED CONTROL SPECIMENS

Sample Number	Ultimate Tensile Strength (MPa)	Sample Number	Bend Angle (deg)
1	131.2	2	> 90
3	128.6	4	> 90
5	130.4	6	> 90
7	129.2	8	> 90
9	131.6	10	> 90

Subjecting the friction weld to the same analysis as the inertia weld, the possible solid-state, volume diffusion can be calculated. Assuming that the maximum temperature during welding approaches the melting point of aluminum (660° C) and a welding-cycle time of 0.5 second for the microfriction welder, diffusion of 400 nm of iron and 24 nm of chromium into aluminum is possible. Therefore, extremely long welding times would be necessary for solid-state, volume diffusion to be a satisfactory explanation for the iron and chromium penetration which was detected. Thus, evaluation of the friction welds coincides with that of the inertia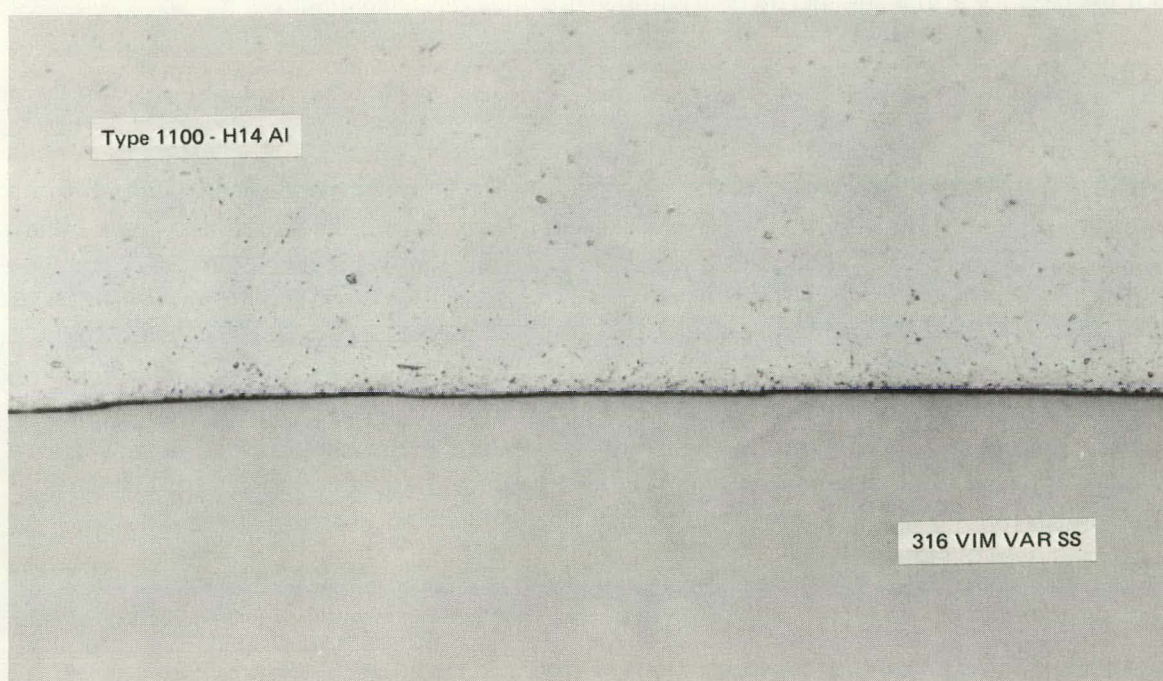 welds. Again, the equivalent penetration of iron and chromium into the aluminum would tend to indicate that possibly mechanical mixing is a satisfactory explanation for the bonding mechanism. However, while it seems reasonable

MS-77-0405-1

Figure 11. PHOTOMACROGRAPH OF THE TYPE 1100-H14 ALUMINUM/316 VIM VAR STAINLESS STEEL FRICTION WELD. (The Hole in the 316 Stainless Steel was not Exposed during Polishing; As Polished; Bright Field Illumination; 4X)

MS-77-0405-3

Figure 12. INTERFACE OF A TYPE 1100-H14/316 VIM VAR STAINLESS STEEL FRICTION WELD (As Polished; Bright Field Illumination; 500X)
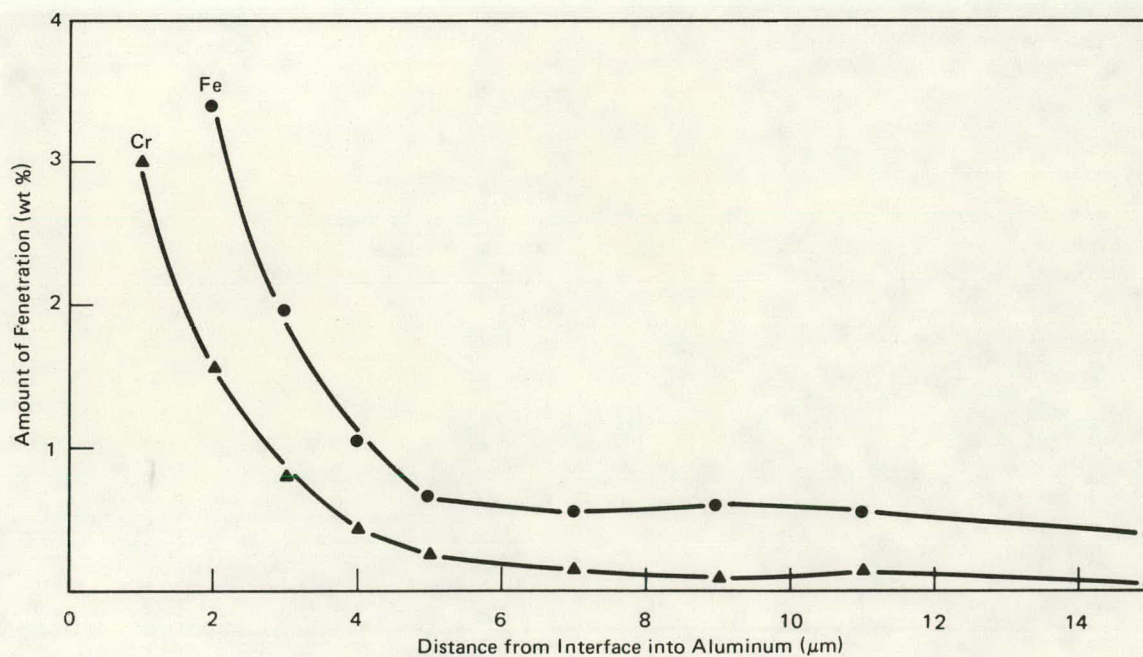

Figure 13. RESULTS OF MICROPROBE SCANS OF THE INTERFACE OF A TYPE 1100-H14 ALUMINUM/316 VIM VAR STAINLESS STEEL FRICTION WELD. (Zero Distance is the Approximate Weld Interface)

to expect some degree of mechanical mixing to be detected by optical microscopy, this was not the case for either the inertia or friction welds that were examined.

CONCLUSIONS

Results of this evaluation of friction and inertia welding indicate that welds can be made between 1100 aluminum and 316 stainless steel. From a purely mechanical standpoint, the strength of these bonds will consistently exceed the strength of the aluminum base metal. However, 100 percent bonding was not reliably achieved and this fact points out the need for nondestructive testing methods to ascertain the degree of bonding. While nondestructive testing of dissimilar metal joints has been encouraging, the work has yet to reach fruition.

This evaluation did not shed much light on a possible bonding mechanism for friction and inertia welding. It does appear that solid-state, volume diffusion is not a satisfactory explanation and that mechanical mixing might be more likely. However, no evidence of mechanical mixing was detected. Additionally, no evidence of melting, as recently reported by others, was detected.

REFERENCES

1. American Welding Society; *Welding Handbook*, 6th Edition, Section 3A, p 503.

2. Wang, K. K.; "Friction Welding", *Welding Research Council, Bulletin 204*; April 1975.

3. *Inertia Welding-Application Principles*; Manufacturing Technology, Inc (1976).

4. Armstrong, R. E.; Lawrence Livermore Laboratory; *Personal Conversation*.

5. Jessop, T. J.; *Friction Welding of Dissimilar Metal Combinations: Aluminum and Stainless Steel*, The Welding Institute Research Report, P/73/75; November 1975.

6. Dinsdale, W. O.; "Dissimilar Metal Joints: How Good are They?", *The Welding Institute Research, Bulletin 17*, (1), p 10 (1976).

7. *Ibid*, p 11.

8. Wang; *Op Cit*, pp 11 - 12.

9. Hood, G. M.; "The Diffusion of Iron in Aluminum", *Philosophical Magazine, 21*, (170), p 305 (1970).

10. Tiwari, G. P. and Sharma, B. D.; "Diffusion of Iron in Aluminum", *Philosphical Magazine, 24*, (189), p 739 (1971).

11. Perkins, R. A., Oak Ridge National Laboratory; *Personal Conversation*.

12. Wang, K. K. and Wen Lin; "Flywheel Friction Welding Research", *The Welding Journal, 53*, (6), Research Supplement, pp 233-S to 241-S (1974).

13. Jessop; *Op Cit*, p 12.

14. Dinsdale, W. O. and Nicholar, E. D.; *Friction Welding of Dissimilar Metal Combinations: Aluminum Alloy HE9 to Stainless Steel*, The Welding Institute Research Report 22/1976/P; December 1976.

15. Kreye, H.; "Melting Phenomena in Solid State Welding Processes", *The Welding Journal, 56*, (5), Research Supplement, pp 154-S to 158-S (1977).

ACKNOWLEDGEMENTS

Distribution

Department of Energy - Oak Ridge

Hickman, H. D.
Leed, R. E.
Zachry, D. S., Jr

Lawrence Livermore Laboratory

Armstrong, R. E.
Mara, G. L.
Nelson, W. E.

Los Alamos Scientific Laboratory

Hoyt, H. C.

Oak Ridge Gaseous Diffusion Plant

Stief, S. S.
Wilcox, W. J., Jr

Oak Ridge National Laboratory

Weir, J. R., Jr

Oak Ridge Y-12 Plant

Alvey, H. E.
Armstrong, R. C.
Bennett, R. K., Jr
Bernander, N. K.
Bieber, C. R.
Burditt, R. B.
Cuddy, L. M.
Cunningham, J. M.
Dodson, W. H./Googin, J. M.
Duggan, H. G.
East, H. C.
Fraser, R. J.
Garrison, M. C.
Gritzner, V. B.
Jackson, V. C.
Jones, F. W.
Kahl, K. G.
Keith, A.
Kite, H. T.
Koger, J. W.
Mason, D. L.
Mills, J. M., Jr
Perkins, M. A. (25)

Phillips, L. R.
Smith, H. F., Jr
Smith, R. D.
Stoner, H. H.
Tewes, W. E.
Tilson, F. V.
Walker, L. R.
Y-12 Central Files (master copy)
Y-12 Central Files (route copy)
Y-12 Central Files (Y-12RC)
Y-12 Central Files (5)

Paducah Gaseous Diffusion Plant

Bewley, H. D.

Union Carbide Corporation - New York

Tinsley, S. W.

In addition, this report is distributed in accordance with the Category UC-38, Engineering and Equipment, as given in the *USERDA Standard Distribution Lists for Unclassified Scientific and Technical Reports*, TID-4500.